

# Ionic Transport in Glassy Networks with High Electronic Polarizabilities: Conductivity Spectroscopic Results Indicating a Vacancy-Type Transport Mechanism

Sevi Murugavel and Bernhard Roling\*

*Institut für Physikalische Chemie und Sonderforschungsbereich 458 (DFG),  
Westfälische Wilhelms-Universität Münster, Corrensstr. 30, 48149 Münster, Germany*

*Received: July 30, 2003; In Final Form: December 17, 2003*

We have carried out ac conductivity measurements on different alkali tellurite and silver halide containing glasses exhibiting high electronic polarizabilities. The analysis of the conductivity spectra provides strong evidence that the ionic site energy distributions in these glasses are distinct from those in conventional glasses with low electronic polarizabilities, such as silicate, borate, and phosphate glasses. Our results can be explained by postulating a vacancy-type transport mechanism, i.e., by assuming that a high electronic polarizability of the glassy network leads to a small and temperature-dependent ratio of empty ionic sites to mobile ions.

## Introduction

Ion-conducting glasses and polymers are important materials for the use as solid electrolytes in batteries, fuel cells, and chemical sensors. In these materials, mobile ions perform thermally activated hopping motions in an amorphous, or at least, highly disordered matrix. Because of the lack of structural information, the understanding of ion dynamics and transport is a difficult task. In contrast to ionic crystals, there is only little information about the number of sites that are available to the mobile ions and about the potential energy of the ions on these sites. Therefore, a variety of different theoretical approaches have been put forward using different assumptions about ion–network and ion–ion interactions.<sup>1–14</sup>

Recently, however, considerable experimental and theoretical progress has been made in the field of ion-conducting glasses regarding the relationships between structure and ion dynamics. Adams and Swenson have used reverse Monte Carlo models of ion-conducting glasses, which were mainly based on X-ray and neutron diffraction data and have applied the bond–valence method in order to obtain information about the structure of the diffusion pathways available to the mobile ions.<sup>15,16</sup> They were able to establish an empirical relation between the pathway volume and the experimentally determined diffusivity of the ions. Several theoretical groups have used molecular dynamics simulations in order to analyze the relationship between glass structure, number of available ionic sites, pathway structure, and ion transport. The results of these simulations provide evidence that the ion transport in glasses can be described in terms of a concept that is well known from ionic crystals, namely, the diffusion of interstitial ions and vacancies. Cormack et al. carried out molecular dynamics simulations on a 0.25Na<sub>2</sub>O•0.75SiO<sub>2</sub> glass and analyzed the sodium-ion migration mechanism.<sup>17</sup> They found that the glass network contains a small number of empty sodium sites that play an important role for the sodium-ion transport. Consequently, they used the term “vacancy-like diffusion mechanism”. Lammert et al. supported these results by completely identifying the ionic sites in molecular dynamics glasses of compositions 0.1Li<sub>2</sub>O•0.9SiO<sub>2</sub>

and 0.5Li<sub>2</sub>O•0.5SiO<sub>2</sub>.<sup>18</sup> They found that in both glasses, the number of available lithium sites is only a few percent larger than the number of lithium ions. Consequently, they suggested that a theoretical description of the ion transport in terms of mobile vacancies is most appropriate. Dyre put forward the idea of a “native” band gap in the spectrum of the ionic site energies.<sup>19</sup> That means a glass contains “native” ionic sites, the number of which is identical to the number of ions, and “non-native” sites. The energy of the “non-native” sites is separated from the energies of the “native” sites by a gap. This idea is based on very general assumptions about ion–network and ion–ion interactions and implies that the ion transport takes place via interstitial ions and vacancies.

To check the validity of these ideas and concepts for real ionic glasses, it seems important to analyze the information about the ion dynamics that can be obtained from spectroscopic techniques, such as conductivity spectroscopy. Conductivity spectra of ion-conducting glasses can be used to obtain information about the time-dependent displacements of the mobile ions in thermal equilibrium. Via linear response theory, the many-particle displacement function

$$\langle R^2(t) \rangle = \frac{1}{N} \left\langle \left( \sum_{i=1}^N \Delta \mathbf{r}_i(t) \right)^2 \right\rangle \quad (1)$$

with  $\Delta \mathbf{r}_i(t)$  denoting the displacement vector of ion  $i$  at time  $t$  from the original position at time  $t = 0$  is directly related to the real part of the ionic conductivity,  $\sigma'(\nu)$ <sup>20</sup>

$$\langle R^2(t) \rangle = \frac{12k_B T}{N_V q^2 \pi} \int_0^t dt' \int_0^\infty \frac{\sigma'(\nu)}{\nu} \sin(2\pi \nu t') d\nu \quad (2)$$

Here,  $N_V$  is the number density of the mobile ions, while  $q$  denotes their charge.  $k_B$  and  $T$  are Boltzmann's constant and the temperature, respectively. The long-time ion dynamics in solid electrolytes is generally characterized by a long-range diffusion leading to a linear increase of  $\langle R^2(t) \rangle$  with time. However on short time scales,  $\langle R^2(t) \rangle$  increases sublinearly with time due to frequent forward–backward hopping motions of the ions. To obtain information about the ion dynamics on a microscopic level, it is instructive to analyze the value of

\* Author to whom correspondence may be addressed. E-mail: roling@uni-muenster.de.

$\langle R^2(t) \rangle$  where the subdiffusive dynamics passes over into the diffusive dynamics. In Section 3, we will show how such a value, denoted by  $\langle R^2(t) \rangle_{\text{cr}}$ , can be defined.

An alternative displacement function is the mean square displacement of the mobile ions

$$\langle r^2(t) \rangle = \frac{1}{N} \left\langle \sum_{i=1}^N \Delta \mathbf{r}_i^2(t) \right\rangle \quad (3)$$

In solid electrolytes with only one type of mobile ions, the mean-square displacement  $\langle r^2(t) \rangle$  is generally smaller than the many-particle displacement function  $\langle R^2(t) \rangle$ . The reason is that there are correlations between the hopping motions of *different* ions in the sense that different ions hop preferably into the same direction. In the limit of long times, these correlations are characterized by the Haven ratio

$$H_R = \lim_{t \rightarrow \infty} \frac{\langle r^2(t) \rangle}{\langle R^2(t) \rangle} \quad (4)$$

which can be obtained experimentally by measuring both the dc conductivity,  $\sigma_{\text{dc}}$ , and the self-diffusion coefficient of the mobile ions,  $D$ . In the case of ion-conducting glasses,  $D$  is generally determined by means of radiotracer techniques.<sup>21–25</sup>

However, since we do not know the Haven ratio for most of the glasses studied here, we analyze, in the following, the many-particle displacement function  $\langle R^2(t) \rangle$ . The results of this analysis support the idea of a vacancy-type transport mechanism in ionic glasses. In particular, in glasses with high electronic polarizabilities of the network, the number of available ionic sites seems to be small and temperature dependent.

## Experimental Section

For the preparation of the silver halide containing glasses, appropriate amounts of high-purity silver halides,  $\text{AgNO}_3$  and  $\text{B}_2\text{O}_3$ , were melted in a quartz crucible slightly above the respective melting temperatures and kept there for about 20 min. Glass samples were then obtained by pouring the melt into a stainless steel mold.

A sodium phosphate glass of composition  $0.5\text{Na}_2\text{O} \cdot 0.5\text{P}_2\text{O}_5$  was prepared from a high purity ammonium dihydrogen phosphate (ADP) and sodium carbonate mixture. Initially, the mixture was reacted in a Pyrex beaker by slowly raising the temperature to 280 °C and keeping it there for 2 h in order to ensure a complete decomposition of the carbonate. The resulting product was then transferred to a silica crucible and melted at 800 °C under an inert atmosphere for 1 h. Then the melt was quenched into a preheated stainless steel mold.

The preparation of  $x\text{Na}_2\text{O} \cdot (1-x)\text{TeO}_2$  glasses, with  $x = 0.1, 0.2$ , and  $0.3$ , of a  $0.25\text{Na}_2\text{O} \cdot 0.75\text{B}_2\text{O}_3$  glass and of a  $0.25\text{Na}_2\text{O} \cdot 0.75\text{SiO}_2$  glass is described in refs 26–28.

All glasses were annealed 30 K below their respective glass transition temperature for 2 h. Then they were stored in a desiccator. For the electrical conductivity studies, silver/platinum electrodes were sputtered onto each surface of the samples. The conductivities were measured in a frequency range from  $10^{-2}$  to  $10^6$  Hz and at different temperatures using a Novocontrol  $\alpha$ -S high-resolution dielectric analyzer.

## Results

In Figure 1, we present the conductivity spectra of a  $0.1\text{Na}_2\text{O} \cdot 0.9\text{TeO}_2$  glass at different temperatures. The real part of the conductivity,  $\sigma'$ , multiplied by the temperature  $T$  is plotted vs

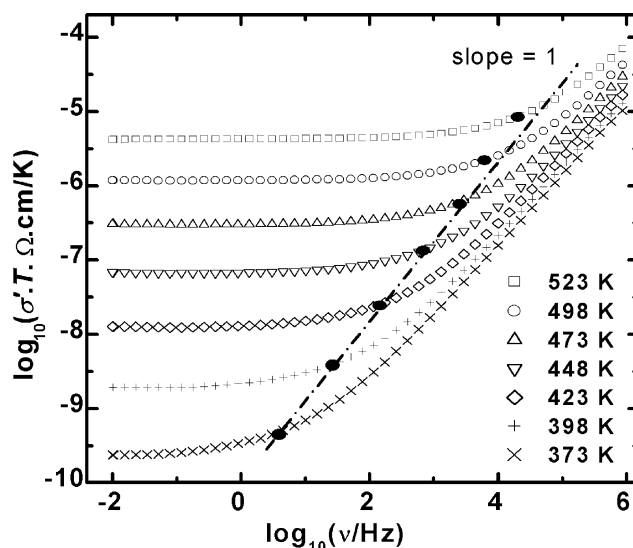


**Figure 1.** Conductivity spectra of a  $0.1\text{Na}_2\text{O} \cdot 0.9\text{TeO}_2$  glass at different temperatures. The real part of the conductivity,  $\sigma'$ , multiplied by the temperature  $T$  is plotted vs frequency  $\nu$ . The filled circles denote the transition points from dc conductivity to dispersive conductivity. The dashed line is a line with a slope of 1. Clearly, the transition points do not lie on this dashed line.

frequency  $\nu$ . At all temperatures, the transition point from dc conductivity  $\sigma_{\text{dc}}$  to dispersive conductivity is marked by a filled circle. The transition frequency  $\nu^*$  was defined by  $\sigma'(\nu^*) = 2\sigma_{\text{dc}}$ .

For many glasses, the transition points lie on a straight line with a slope of 1, i.e., the transition frequency  $\nu^*$  is activated with the same thermal activation energy as the dc conductivity  $\sigma_{\text{dc}}$ .<sup>26</sup> Together with the finding that the shape of the spectra is independent of temperature (time–temperature superposition principle (TTSP)), this implies that the value of the many-particle displacement function  $\langle R^2(t) \rangle$  at the transition from subdiffusive dynamics to diffusive dynamics

$$\langle R^2(t) \rangle_{\text{cr}} = \langle R^2(t^*) \rangle \quad (5)$$

with

$$t^* = \frac{1}{2\pi\nu^*}$$

is independent of temperature. This was shown in detail in ref 29. In the case of the  $0.1\text{Na}_2\text{O} \cdot 0.9\text{TeO}_2$  glass, the TTSP is valid; however, the transition point does *not* lie on a line with a slope of 1. From this, it follows that  $\langle R^2(t) \rangle_{\text{cr}}$  depends on temperature. The temperature dependence can be described by a power law

$$\langle R^2(t) \rangle_{\text{cr}} \propto T^\beta \quad (6)$$

with  $\beta = 2.3$ .<sup>28</sup> For sodium tellurite glasses  $x\text{Na}_2\text{O} \cdot (1-x)\text{TeO}_2$ , the temperature exponent  $\beta$  decreases with increasing sodium oxide content  $x$ .<sup>28</sup>

One important property of tellurite glasses is an unusually high refractive index, i.e., an unusually high electronic polarizability of the glass network. The main reason for this high polarizability is the lone pairs of electrons at the tellurium atoms; see the schematic illustration of the structure of tellurite glasses in Figure 2. With increasing sodium oxide content, the number density of these lone pairs, and thus the electronic polarizability, decreases. This suggests that the decrease of the exponent  $\beta$

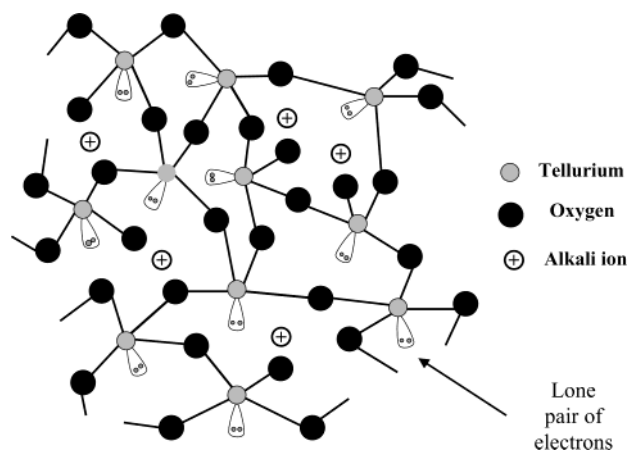


**Figure 2.** Schematic illustration of the structure of alkali tellurite glasses. The lone pairs of electrons at the tellurium atoms cause the high electronic polarizability of these glasses.

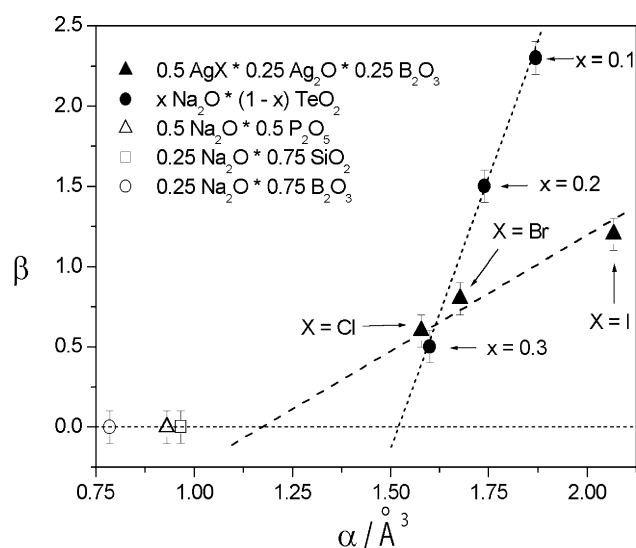


**Figure 3.** Plot of the exponent  $\beta$  vs the average electronic polarizability per atom/ion,  $\alpha$ . Glasses with low electronic polarizabilities are characterized by a temperature-independent value of  $\langle R^2(t) \rangle_{cr} \propto T^\beta$ . On the other hand, for glasses with high electronic polarizabilities,  $\langle R^2(t) \rangle_{cr} \propto T^\beta$  increases with temperature  $T$ .

with increasing  $x$  is related to the decrease of the electronic polarizability.

This is supported by measurements on  $0.5\text{AgX} \cdot 0.25\text{Ag}_2\text{O} \cdot 0.25\text{B}_2\text{O}_3$  glasses. In Figure 3, we plot the exponent  $\beta$  vs the average electronic polarizability per atom or ion,  $\alpha$ , of different glasses. Values for  $\alpha$  were calculated from the refractive indices<sup>30–32</sup> using the Clausius–Mosotti equation. In the case of the  $x\text{Na}_2\text{O} \cdot (1-x)\text{TeO}_2$  glasses, we find a linear relation between  $\beta$  and  $\alpha$ . Similarly, in the case of the  $0.5\text{AgX} \cdot 0.25\text{Ag}_2\text{O} \cdot 0.25\text{B}_2\text{O}_3$  glasses with  $X = \text{Cl}, \text{Br}, \text{and I}$ , the exponent  $\beta$  increases with the polarizability  $\alpha$ , but the average slope  $\Delta\beta/\Delta\alpha$  is smaller than for the tellurite glasses; see the dashed lines in Figure 3. When these dashed lines are extrapolated to  $\beta = 0$ , polarizability values between  $1.15 \text{ \AA}^3$  and  $1.5 \text{ \AA}^3$  are obtained. Many conventional glassy electrolytes, such as alkali silicate, borate, and phosphate glasses, are characterized by lower polarizability values. In Figure 3 we show, exemplarily, three data points for a  $0.25\text{Na}_2\text{O} \cdot 0.75\text{B}_2\text{O}_3$  glass with  $\alpha = 0.79 \text{ \AA}^3$ , a  $0.5\text{Na}_2\text{O} \cdot 0.5\text{P}_2\text{O}_5$  glass with  $\alpha = 0.93 \text{ \AA}^3$ , and a  $0.25\text{Na}_2\text{O} \cdot 0.75\text{SiO}_2$  glass with  $\alpha = 0.97 \text{ \AA}^3$ . For these three glasses, the exponent  $\beta$  is zero. These results

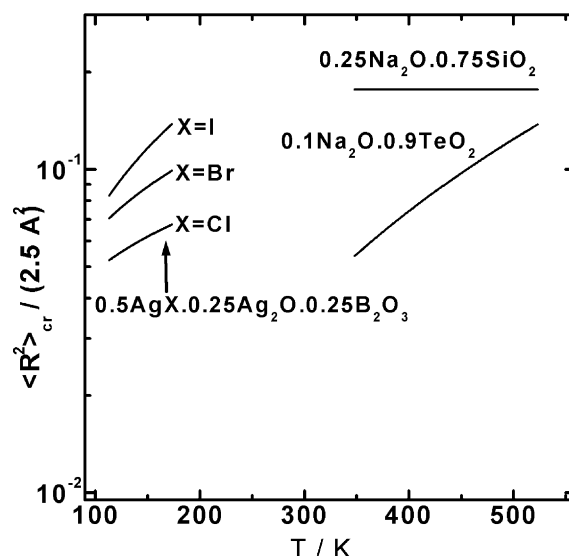


**Figure 4.** Plot of the normalized quantity  $\langle R^2(t) \rangle_{cr} / (2.5 \text{ \AA})^2$  vs temperature  $T$  for different glasses. Note that for glasses with high electronic polarizabilities, such as the  $0.1\text{Na}_2\text{O} \cdot 0.9\text{TeO}_2$  glass and the  $0.5\text{AgX} \cdot 0.25\text{Ag}_2\text{O} \cdot 0.25\text{B}_2\text{O}_3$  glasses, the values of the normalized quantity  $\langle R^2(t) \rangle_{cr} / (2.5 \text{ \AA})^2$  are remarkably small. This implies that at the transition from subdiffusive ion dynamics to diffusive ion dynamics, only a small fraction of the ions has left their original sites.

show clearly that the electronic polarizability plays an important role for the mechanism of the ion transport.

In Figure 4 we plot the normalized quantity  $\langle R^2(t) \rangle_{cr} / (2.5 \text{ \AA})^2$  vs temperature for different glasses with high and low electronic polarizabilities.  $2.5 \text{ \AA}$  is an estimate for a jump distance between neighboring positions in the glass network. This estimate is in agreement with jump distances found in molecular dynamics simulations.<sup>33,34</sup> If one assumes that there are no jumps over shorter distances, then  $\langle R^2(t) \rangle_{cr} / (2.5 \text{ \AA})^2$  represents an *upper limit* for the fraction of mobile ions that have left their original sites at the transition from subdiffusive to diffusive dynamics. As seen from Figure 4, this fraction is of the order of a few percent for the  $0.1\text{Na}_2\text{O} \cdot 0.9\text{TeO}_2$  glass and the  $0.5\text{AgX} \cdot 0.25\text{Ag}_2\text{O} \cdot 0.25\text{B}_2\text{O}_3$  glasses, and it increases with temperature. For glasses with low polarizabilities, such as the  $0.25\text{Na}_2\text{O} \cdot 0.75\text{SiO}_2$  glass with  $\alpha = 0.97 \text{ \AA}^3$ , the fraction is higher and independent of temperature.

## Discussion

Our results show that the ion dynamics in glasses with high electronic polarizabilities are characterized by remarkably small values of  $\langle R^2(t) \rangle_{cr}$ . That means that only a small fraction of ions have moved away from their original sites when the subdiffusive dynamics passes over into the diffusive dynamics. One possibility to explain this observation is to propose a vacancy-type transport mechanism as has recently been done by Cormack et al., Lammert et al., and Dyre.<sup>17–19</sup> Let us therefore assume now that the ion transport is strongly influenced by a small number of empty ionic sites, and let us call these empty ionic sites “vacancies”. For the calculation of conductivity spectra, it is sufficient to consider the dynamics of vacancies. The vacancy dynamics determine the movements of the center of charge and thus the frequency-dependent conductivity. Because of the disorder of the glassy network and the Coulomb interactions between the vacancies, the short-time vacancy dynamics will be subdiffusive, while the long-time dynamics will be diffusive. At the transition from the subdiffusive dynamics to the diffusive dynamics, the value of the vacancy displacement function, which



will, in the following, be denoted by  $\langle R^2(t) \rangle_{\text{cr,vacancies}}$ , should be at least a few jump distances squared. On shorter-length scales, the vacancy dynamics will be slowed by the disorder of the glass network.

Now it is important to realize that the experimentally determined value of  $\langle R^2(t) \rangle_{\text{cr}}$  is averaged over *all ions* in the sample. This value is given by

$$\langle R^2(t) \rangle_{\text{cr}} = \langle R^2(t) \rangle_{\text{cr,vacancies}} \frac{N_{\text{vacancies}}}{N_{\text{ions}}} \quad (7)$$

Thus, our experimental results suggest that for glasses with high electronic polarizabilities, the ratio of the number of vacancies to the number of ions is small and temperature dependent. At low temperatures, the number of available empty sites is small, but with increasing temperature, more sites become available. The number of available sites, and its variation with temperature, depends, of course, on the distribution of site energies in a glass. Thus, this distribution seems to be strongly influenced by the electronic polarizability of the glass network. To obtain a better understanding of this influence, it seems important to carry out molecular dynamics simulations on glasses with different electronic polarizabilities and to analyze the distribution of site energies and the resulting temperature dependence of  $\langle R^2(t) \rangle_{\text{cr}}$ . Here it is important to note that the lithium silicate glasses studied by Lammert et al. in their molecular dynamics simulations are glasses with *low* electronic polarizabilities.<sup>18</sup> Nevertheless, the number of lithium sites is only a few percent larger than the number of ions. Our results suggest that the ratio of empty sites to mobile ions is even smaller in glasses with high electronic polarizabilities.

In this context, it is interesting to consider the Almost and West formalism that is often used to determine the number density of mobile ions in solid electrolytes.<sup>35,36</sup> For many crystalline and glassy conductors, the application of this formalism results in a temperature-independent number density of mobile ions, but there are some examples of temperature-dependent number densities. In particular, Pan and Ghosh<sup>37,38</sup> found a number density that increases with temperature in the case of lithium ion conducting bismuthate and lead bismuthate glasses. Remarkably, these glasses exhibit high electronic polarizabilities of the network. Therefore, the results of Pan and Ghosh are closely related to ours. However, it is important to note that the Almond and West formalism does *not* yield the number density of mobile ions that contributes to the dc conductivity but gives an estimate of the fraction of ions that has moved at the crossover time from subdiffusive to diffusive dynamics. This is because in the framework of this formalism, the crossover frequency from dc to dispersive conductivity is used for the calculation of the number density. Thus, the “fraction of mobile ions” determined by the Almond and West formalism should be similar to our normalized quantity  $\langle R^2(t) \rangle_{\text{cr}}/(2.5 \text{ \AA})^2$ .

Finally, we would like to point, once again, to an interesting feature in Figure 3. In the case of the silver halide silver borate glasses, the increase of the exponent  $\beta$  with the polarizability  $\alpha$  is less pronounced than for the alkali tellurite glasses. The reason for this finding is not clear at present. One possible explanation is that the high electronic polarizability of silver ions as compared to alkali ions makes them less susceptible to the electronic polarizability of the glass network. This hypothesis will be checked by further experiments.

## Conclusions

We have studied the influence of the electronic polarizability of a glass network on ion dynamics and transport. When the average polarizability per atom/ion in a glass exceeds values of about  $1.5 \text{ \AA}^3$ , the normalized quantity  $\langle R^2(t) \rangle_{\text{cr}}/(2.5 \text{ \AA})^2$  becomes small and temperature dependent. This can be explained in the framework of a vacancy-type transport mechanism, i.e., by assuming that, at low temperatures, the ratio of empty ionic sites to mobile ions is small but increases with temperature. Thus, our results suggest that the electronic polarizability of a glass network strongly influences the *distribution* of ionic site energies.

**Acknowledgment.** We are indebted to M. D. Ingram for many stimulating discussions and to S. Pas for critically reading the manuscript. Furthermore, we would like to thank the Deutsche Forschungsgemeinschaft for financial support of this work via the SFB 458.

## References and Notes

- (1) Bunde, A.; Maass, P. *Physica A* **1993**, *200*, 80.
- (2) Bunde, A.; Ingram, M. D.; Maass, P. *J. Non-Cryst. Solids* **1994**, *172–174*, 1222.
- (3) Dieterich, W.; D. Knödler, Pendzig, P. *J. Non-Cryst. Solids* **1994**, *172–174*, 1237.
- (4) Baranovskii, S. D.; Cordes, H. *J. Chem. Phys.* **1999**, *111*, 7546.
- (5) Pendzig, P.; Dieterich, W.; Nitzan, A. *J. Non-Cryst. Solids* **1998**, *235*, 748.
- (6) Dyre, J. C.; Schroder, T. B. *Rev. Mod. Phys.* **2000**, *72*, 873.
- (7) Schroder, T. B.; Dyre, J. C. *Phys. Rev. Lett.* **2000**, *84*, 310.
- (8) Roling, B. *Phys. Chem. Chem. Phys.* **2001**, *3*, 5093.
- (9) Funke, K.; Heimann, B.; Vering, M.; Wilmer, D. *J. Electrochem. Soc.* **2001**, *148*, A395.
- (10) Funke, K.; Banhatti, R. D.; Bruckner, S.; Cramer, C.; Wilmer, D. *Solid State Ionics* **2002**, *154*, 65.
- (11) Kirchheim, R. *J. Non-Cryst. Solids* **2000**, *272*, 85.
- (12) Paulmann, D.; Kirchheim, R. *J. Non-Cryst. Solids* **2001**, *286*, 210.
- (13) Durr, O.; Dieterich, W.; Nitzan, A. *Solid State Ionics* **2002**, *149*, 125.
- (14) Ingram, M. D.; Roling, B. *J. Phys.: Condens. Mater.* **2003**, *15*, S1595.
- (15) Adams, S.; Swenson, J. *Phys. Chem. Chem. Phys.* **2002**, *4*, 3179.
- (16) Swenson, J.; Adams, S. *Phys. Rev. Lett.* **2003**, *90*, 155507.
- (17) Cormack, A. N.; Du, J.; Zeitler, T. R. *Phys. Chem. Chem. Phys.* **2002**, *4*, 3193.
- (18) Lammert, H.; Kunow, M.; Heuer, A. *Phys. Rev. Lett.* **2003**, *90*, 215901.
- (19) Dyre, J. C. *J. Non-Cryst. Solids* **2003**, *324*, 192.
- (20) Roling, B.; Martiny, C.; Brückner, S. *Phys. Rev. B* **2001**, *63*, 214203.
- (21) Kelly, J. E., III; Cordaro, J. F.; Tomozawa, M. *J. Non-Cryst. Solids* **1980**, *41*, 47.
- (22) Kelly, J. E., III; Tomozawa, M. *J. Non-Cryst. Solids* **1982**, *51*, 345.
- (23) Thomas, M. P.; Peterson, N. L. *Solid State Ionics* **1984**, *14*, 307.
- (24) Kahnt, H. *J. Non-Cryst. Solids* **1996**, *203*, 225.
- (25) Imre, A. W.; Voss, S.; Mehrer, H. *Phys. Chem. Chem. Phys.* **2002**, *4*, 3219.
- (26) Roling, B.; Happe, A.; Funke, K.; Ingram, M. D. *Phys. Rev. Lett.* **1997**, *78*, 2160.
- (27) Roling, B.; Ingram, M. D. *Phys. Rev. B* **1998**, *57*, 14192.
- (28) Murugavel, S.; Roling, B. *Phys. Rev. Lett.* **2002**, *89*, 195902.
- (29) Roling, B.; Funke, K. *Recent Res. Dev. Non-Cryst. Solids* **2002**, *2*, 299.
- (30) Terashima, K.; Hashimoto, T.; Yoko, T. *Phys. Chem. Glasses* **1996**, *37*, 129.
- (31) Kim, S.-H. *J. Mater. Res.* **1999**, *14*, 1074.
- (32) Dimitrov, V.; Komatsu, T. *J. Non-Cryst. Solids* **1999**, *249*, 160.
- (33) Balasubramanian, S.; Rao, K. J. *J. Non-Cryst. Solids* **1995**, *181*, 157.
- (34) Heuer, A.; Kunow, M.; Vogel, M.; Banhatti, R. D. *Phys. Chem. Chem. Phys.* **2002**, *4*, 3185.
- (35) Almond, D. P.; Duncan, G. K.; West, A. R. *Solid State Ionics* **1983**, *8*, 159.
- (36) Almond, D. P.; West, A. R. *Solid State Ionics* **1983**, *9 & 10*, 277.
- (37) Pan, A.; Ghosh, A. *Phys. Rev. B* **2000**, *62*, 3190.
- (38) Pan, A.; Ghosh, A. *J. Chem. Phys.* **2000**, *112*, 1503.